Numerical Simulation of Piles Subjected To Lateral Spreading and Comparison with Shaking Table Results

Asaadi, A.[1*], Sharifipour, M.[2] and Ghorbani, K.[1]

[1] M.Sc., Department of Civil Engineering, Faculty of Engineering, Razi University, Kermanshah, Iran.
[2] Assistant Professor, Department of Civil Engineering, Faculty of Engineering, Razi University, Kermanshah, Iran.

ABSTRACT: Pile foundations are relatively vulnerable to lateral loads. During liquefaction-induced lateral spreading, this vulnerability is particularly conspicuous due to a loss of strength and stiffness in the liquefied soil. A nonlinear effective stress analysis incorporating an elastoplastic constitutive model based on Finite Difference Method (FLAC[2D] program) was used to numerically simulate shake table experiment on piles in laterally spreading soils. The soil-pile interaction has been properly considered by using interface elements. The main objective of this paper is to assess the accuracy of a 2D numerical simulation of physical models in predicting the dynamic response of pile foundations and to identify the capability of 2D numerical simulation for 3D effects such as shadow and neighboring effects in pile groups without a pile cap. Results are presented and discussed, in which the obtained response from the simulation is compared to that measured in the test. For the single pile, a fairly good agreement was observed between computed and measured results. It was also found that the shadow and neighboring effects reduced lateral load on the piles by few percent of difference compared with experimental results.

Keywords: FLAC[2d], Lateral Spreading, Liquefaction, Numerical Simulation, Soil-Pile Interaction.

INTRODUCTION

The prediction of liquefaction and resulting displacements is a major concern for earth structures located in regions of moderate to high seismicity (Byrne et al., 2004). Previous case histories show that liquefaction-induced large lateral displacement imposed severe damages to many structures supported on pile foundations during earthquakes. The loss of strength and stiffness of soil due to liquefaction may cause large bending moments and shear forces in piles embedded in liquefying grounds. This is particularly so for sloping grounds that permanent horizontal displacements can occur during liquefaction imposing significant kinematic loads on pile foundation and inflict severe damages. In the 1964 Niigata earthquake, lateral spreading caused the failure of the Showa Bridge, when a 10-m layer of liquefied soil moved towards the Shinano River (Abdoun et al., 2005). During the 1995 Kobe earthquake, a three story RC building tilted by 5° due to pile

* Corresponding author E-mail: asaadi.edu@gmail.com

damage caused by lateral spreading where the permanent horizontal ground displacement was 2 m at the quay wall and 0.8 m at the pile heads (Tokimatsu et al., 1997).

Prediction of seismic response of pile foundations in liquefying soil layers is difficult and there are many uncertainties in the mechanisms involved in soil structure interaction (Rahmani and Pak, 2012). A wide range of research works have been implemented for evaluation of pile foundations response in liquefying grounds, including centrifuge and shaking table tests (Wilson, 1998; Tokimatsu et al., 2005; Towhata et al., 2006; He et al., 2008; Su et al., 2015) and also various numerical modeling (Cheng and Jeremić, 2009; Rahmani and Pak, 2012; Chang et al., 2013; Karimi and Dashti, 2015; Asaadi and Sharifipour, 2015). Despite the wide range of studies, as regards to the efficiency and power of numerical simulation tools, there is so interest to provide more insight in this subject.

Dealing with large-scale physical models such as shake table tests, is thought to be difficult, therefore, numerical modeling may be an efficient tool for dynamic geotechnical studies considering some complex features such as soil-structure interaction. This cannot be realized unless it proves to be valid when comparing numerical results to measured experiments. Validation is the assessment of the accuracy of a computational simulation by comparison with experimental data (Oberkampf et al., 2004). Current study aims to assess the accuracy and capability of an effective stress analysis by using a 2D plane strain Finite Difference program, in predicting the response of piles to lateral spreading. Results of a shake table test conducted by Haeri et al. (2012) in the Earthquake Research Center at Sharif University of Technology (SUT) are used for this validation. In this paper, 2D simulation of 3D effects such as shadow and neighboring effects is also evaluated.

DESCRIPTION OF THE EXPERIMENT

A brief description of the shaking table test is given here for completeness. The rigid container (box) used in the test has dimensions of 3.5 m length, 1.0 m width, and 1.5 m height. In contrary to dynamic soil-structure interaction problems in physical modeling, rigid boundary condition in this test was of low degree of importance as the phenomenon has been studied was rather kinematic in nature (no inertial load representing superstructure loads were existed).

The ground in the model consisted of a 1-m thick liquefiable sand layer with a relative density of 15%, overlying a non-liquefiable sand layer having a relative density of 80%. The slope of the soil layers was about 4° in longitudinal direction. Figure 1 shows the schematic cross section and plan view of the physical model along with the general layout of transducers. As shown in this figure, the physical model consisted of six piles configured in three separate series. The piles were made of aluminum pipes with outer diameter of 5.0 cm, 0.26 cm wall thickness, and 1.25 m of height. All piles were fixed-end type piles. Piles 1 and 2, as front and shadow piles, were aligned in the direction of lateral spreading to study shadowing effect, while piles 4, 5 and 6 formed a set of three piles aligned in a row perpendicular to the direction of lateral spreading to study the neighboring effect. Pile 3 also acted as a single pile.

In the test, all required parameter of the physical model were scaled using similitude law suggested by Iai et al. (2005). Considering the dimensions of the rigid box, a geometric scale of λ=8 was used and introduced. Detailed information about scaling factors is available in Haeri et al. (2012). The model was shaken with a sinusoidal base acceleration having a frequency of 3.0 Hz and amplitude of 0.2 g with 12 seconds in duration (Figure 2).
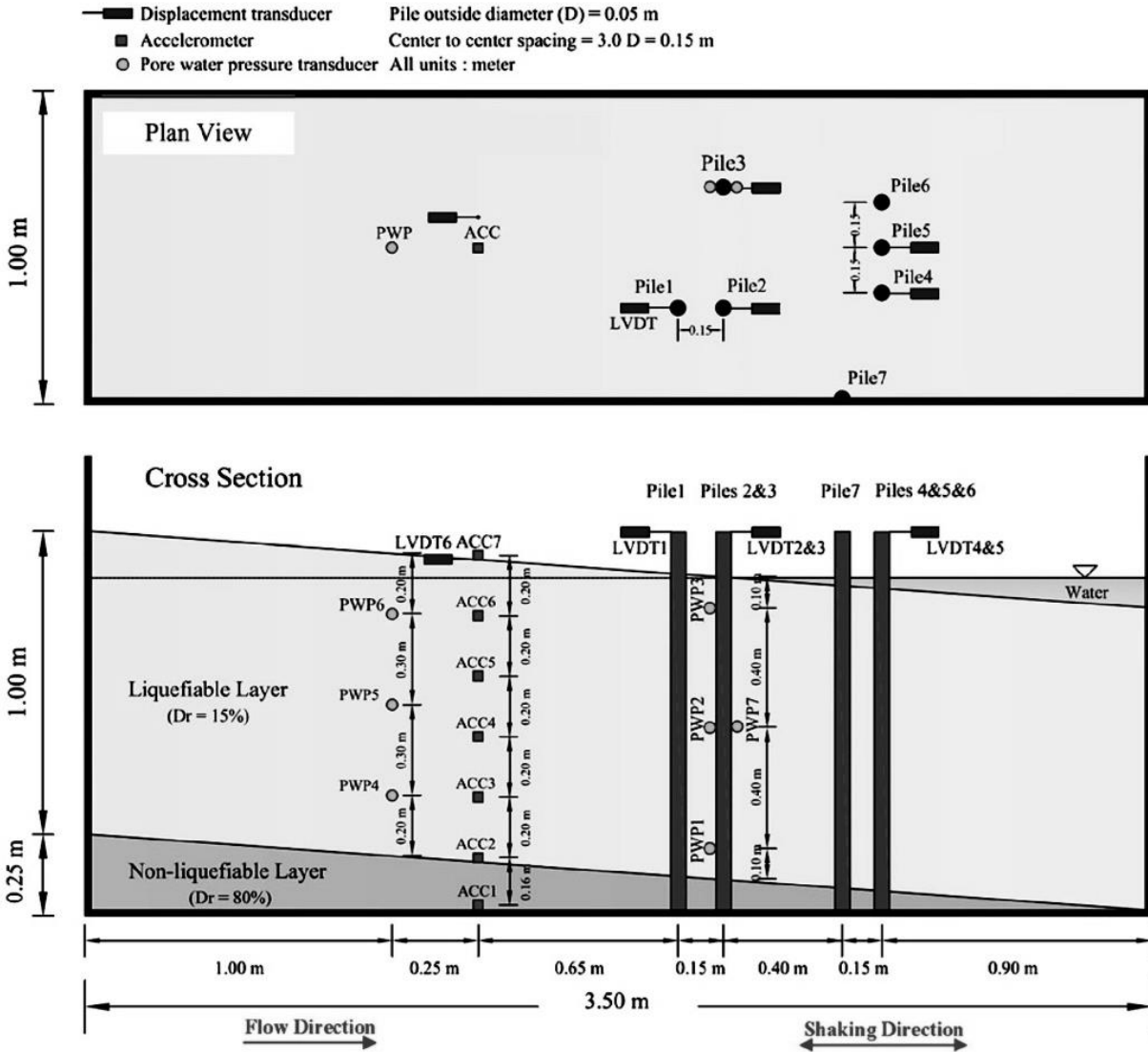
Fig. 1. Plan view and cross section of the physical model and the location of installed instruments in the test by Haeri et al. (2012)
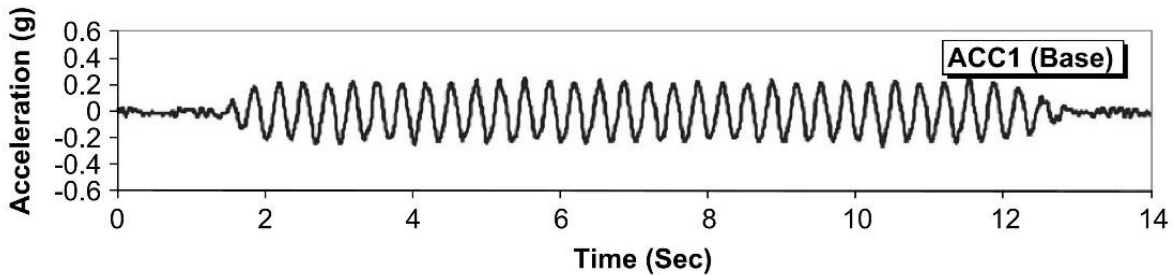

Fig. 2. Acceleration time history of the base excitation in the test (Haeri et al., 2012)

METHOD OF ANALYSIS AND SIMULATION PROCEDURE

The numerical simulations are carried out using the plane strain Finite Difference program, FLAC^{2D} (Itasca Consulting Group, 2011). The physical model geometry and material properties are transformed to the

prototype scale. The lateral dimension is adopted as 28 m and the height of the model is 12 m and 10 m for left and right sides, respectively. Total soil medium is discretized into 600 Finite Difference meshes in 15 rows and 45 columns and the zones are set finer around the pile for more precision in this area. Each pile is divided into 17 segments with three degrees of freedom at each node (two displacements and one rotation), and is fixed at the bottom in both translational and rotational directions, simulating fixed-end type piles. The number of pile segments is chosen so that the number of embedded ones is equal to the rows of zones in the soil medium. The observation points used in the simulation, are sketched in Figure 3 based on the instrumentations in physical model, which were included: accelerometers (ACCs) and pore water pressure transducers (PWPs) in free field (far from the piles) and close to the single pile (pile 3) to record soil accelerations and build-up/dissipation of excess pore water pressures, respectively, and displacement transducers (LVDTs) at the

uppermost pile node (pile head) as well as the free field ground surface to record pile and soil lateral displacements, accordingly. The pore water pressure in FLAC^{2D} can be calculated in zones; however, acceleration and displacement histories are calculated at grid points.

MATERIAL PROPERTIES

Using a comprehensive constitutive model is one of the most important parts of numerical simulation of dynamic behavior of liquefiable soils (Rahmani and Pak, 2012). In the present study, the soil is modeled using nonlinear elastoplastic Mohr-Coulomb constitutive model, and the piles are modeled using linearly elastic pile elements. The soil properties used in the numerical simulation are outlined in Table 1. However, the material parameters of the soil (Firoozkuh silica sand No. 161) required for the computer program are more than those given in the experimental work by Haeri et al. (2012).
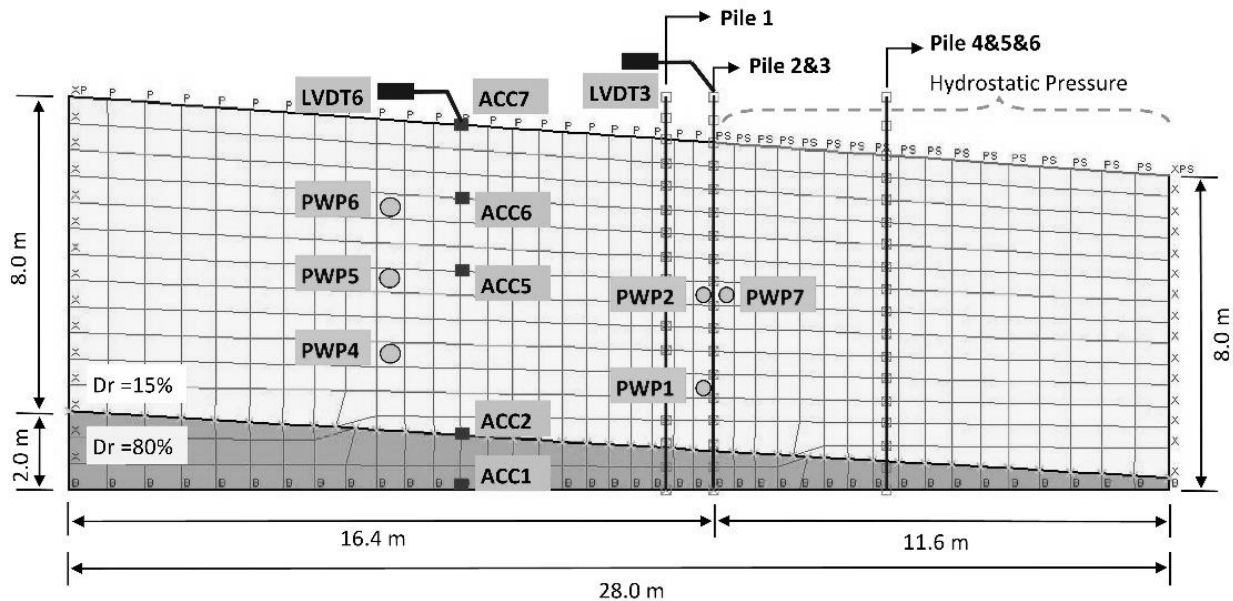

Fig. 3. Model geometry, Finite Difference mesh, and the instrumentations layout of the test simulated in FLAC^{2D}

Table 1. Material properties of soil (Firoozkuh silica sand)

Material Parameters	Loose Layer	Dense Layer
Dr (%)	15	80
Saturated Density, ρ_{sat} (kg/m³)	1864	1966
Porosity	0.45	0.38
Friction angle, φ (deg)	20	41
Permeability, k (m/s)	7.46 E-5	3.12 E-5
Low strain Shear Modulus, G (Mpa)	52	90
Low strain Bulk Modulus, K (Mpa)	110	150
$(N_1)_{60}$	3	45
Normal (kn) & Shear (ks) Stiffness, (N/m/m)	29.9 E8	45 E8

Therefore, the rest of them have been adapted from other sources, which have provided data about mechanical properties of this sand, such as Mirlatifi et al. (2007), Dabiri et al. (2011), and Askari et al. (2011). Geometrical and mechanical properties of piles are also summarized in Table 2.

It must be noted that the initial shear modulus, G_{max} (before the seismic loading), is not uniform throughout each material unit, and the variation of shear modulus along the depth of soil profile (with changes in the effective mean normal stress) is taken into account using the following equation given by Popescu and Prevost (1993):

$$G_S = G_0 \left(\frac{\frac{1+2K_0}{3} \sigma'_0}{P_0} \right)^{0.7} \text{MPa} \qquad (1)$$

where, K_0: is the coefficient of lateral earth pressure at rest, P_0: is the reference normal stress that is 100 kPa for sand (Popescu and Prevost, 1993), and G_0: is the low-strain shear modulus of the soil. This variation is initially implemented during the static loading stage by using a *Fish* function.

Soil-pile-interaction effects are also considered employing interface elements available in FLAC^{2D} program. In the present study, the interfaces were modeled via shear (k_s) and normal (k_n) coupling springs, which are selected at approximately ten times the equivalent stiffness of the stiffest neighboring zone (Itasca Consulting Group, 2011):

$$k_n \quad or \quad k_s = 10 \times \max \left[\frac{K + \frac{4}{3}G}{\Delta Z_{min}} \right] \qquad (2)$$

where, K and G: are the bulk and shear modulus of soil zone, respectively, and ΔZ_{min}: is the smallest dimension of an adjoining zone in the normal direction. Since the soil is cohesionless, cohesive strength is not considered in the interface elements but the frictional resistance of the shear and normal coupling springs are set depending on the friction values of the soil around the pile, which reflect the roughness of the pile surface (about 50-70 percent of the soil friction angle) (Itasca Consulting Group, 2011). Table 1 also summarizes the interface stiffness properties used in the simulations after adjustment from values calculated by using Eq. (2).

Table 2. Pile properties (prototype)

Material Parameters	
Diameter (m)	0.4
Pile length (m)	10
Density (equivalent filled), (kg/m³)	6.75
Modulus of Elasticity, E (Mpa)	5.9 E5
Moment of Inertia, I (m⁴)	2.417 E-4
Perimeter (m)	1.257
Cross sectional area, A (m²)	0.1257

DYNAMIC LOADING

The dynamic input load has been applied to the base of the model as a sinusoidal base acceleration, having a frequency of 3.0 Hz and amplitude of 0.2 g, which imitates the test input motion. It has a duration of 12.0 s, which is formulated in equation 3 (plotted in Figure 4). It should be noted that the time and frequency of input load were scaled to prototype according to the scaling factors, and introduced to the program by a *Fish* function during the analysis.

$$
\begin{aligned}
a &= 0.2 \times (t\text{-}1) \times \sin(2\pi f\, t) ; & (1 \le t \le 2) \\
a &= 0.2 \times \sin(2\pi f\, t) ; & (2 \le t \le 12) \\
a &= 0.2 \times (13\text{-}t) \times \sin(2\pi f\, t) ; & (12 \le t \le 13)
\end{aligned}
$$
$$(3)$$

where *a*, *f*, and *t*: are acceleration, frequency, and dynamic time, respectively. For accurate representation of wave transmission through the model, the grid zone size, *Δl*, must be smaller than the value calculated by the following equation (Kuhlemeyer and Lysmer, 1973):

$$\Delta l_{max} = \frac{c_s}{10 f} \qquad (4)$$

where, C_s: is the shear wave velocity of the soil and *f*: is the frequency of the shear wave.

According to the lowest shear wave velocity that is corresponding to the soil with lowest relative density (loose sand upper layer), a maximum admissible zone size of 1 m is considered in the modeling with underestimation.

ANALYSIS APPROACH

Generally, the model analyses have been performed in three phases. First, the soil elements were loaded by geostatic condition, the hydrostatic pressure of the water on the right side of the ground was applied, the piles were placed in the soil, the interface properties were applied, and the model has been analyzed to obtain the natural steady state. These new computed values are used as initial stresses for the next calculations. Then, the model is analyzed in groundwater flow condition. In the static analysis, the soil-pile system was only subjected to gravity loading, the base boundary was fixed in both directions, and the side boundaries were fixed in *x* direction. In contrary to dynamic soil-structure-interaction problems, the free-field boundary condition was not applied to the model since the test was itself accomplished with a rigid box, and this is because of the kinematical nature of the model as mentioned before. Finally, the dynamic analysis is carried out in coupled dynamic-groundwater calculations.
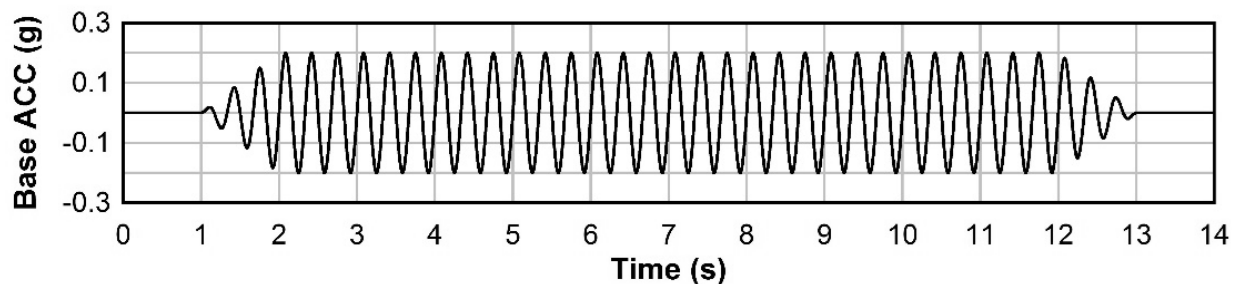

Fig. 4. Acceleration time history of dynamic load used in the simulation

Rayleigh damping was used in the numerical analyses herein. The two terms of Rayleigh damping (mass and stiffness) are both dependent upon frequency, however, it is considered to be frequency-independent over a range of predominant frequencies of a response referred to a typical velocity record. The idea is to try to get the right damping by adjust the center frequency (f_c) of Rayleigh damping, so that its range coincides with the important frequency. For many problems (such as dynamic analysis of underground structures), the important frequency is related to the natural mode of oscillation of the system (Itasca Consulting Group, 2011). In the case of choosing the damping ratio (ξ), since the analysis uses the plasticity constitutive model involve large strain (i.e. Mohr-Coulomb); a considerable amount of energy dissipation can occur during plastic flow. Thus, only a minimal percentage of damping (e.g., 0.5%) may be required (Itasca Consulting Group, 2011). With this background, a damping ratio (ξ_{min}) of 0.05 and center frequency (f_c) equaling 15 Hz (estimated by undamped elastic simulation) is considered.

It should be noted that the model has been analyzed separately in three different series, which is different from that sketched in Figure 3, in terms of construction. First, a model just with pile 3 has been analyzed that is widely taken into investigation, then, the set of pile 1 and pile 2 is analyzed to study shadowing effects, and finally the analysis is carried out for the set of piles 4, 5, and 6, so that they modeled to be aligned in a row perpendicular to the shaking direction to study neighboring effect. The neighboring effect in pile groups is substantially a three-dimensional (3D) issue; regularly spaced piles can be reduced to a 2D problem in analysis by averaging the 3D effects over the distance between piles. (Donovan et al., 1984) suggests that linear scaling of material properties is a simple and convenient way of distributing the discrete effect of elements over the distance between elements in a regularly spaced pattern. The relation between actual and scaled properties can be described by considering the strength properties for regularly spaced piles. The following properties are to be scaled: 1) elastic modulus, 2) stiffness of the normal and shear coupling springs, 3) pile perimeter. The input parameters are given as the actual values divided by the spacing of the piles. The actual pile responses (i.e., forces and moments) are then determined by multiplying the spacing value (Donovan et al., 1984). The mechanism of this scaling is automatically available in FLAC^{2D}. When spacing is specified in the *"structure prop"* command, the actual properties of the structural elements are inputted, the scaled properties are then calculated automatically, and when the calculation is completed, the actual results are then determined (Itasca Consulting Group, 2011).

LIQUEFACTION MODELING

Liquefaction is caused by the tendency of granular soil to condense when subjected to monotonic or cyclic shear loading. When the volume change is prevented or curtailed by the presence of water in the pores, normal stress is transferred from the soil skeleton to the water. This can cause high excess pore pressures resulting in a very large reduction in shear stiffness. This mechanism is well described in the following empirical equation proposed by Byrne (1991):

$$\frac{\Delta\varepsilon_{vd}}{\gamma} = c_1 \exp\left(-c_2 \frac{\varepsilon_{vd}}{\gamma}\right) \qquad (5)$$

where, $\Delta\varepsilon_{vd}$: is the increment of volume decrease, γ: is the cyclic shear-strain, and c_1 and c_2: are constants dependent on the volumetric strain behavior of sand. Byrne

(1991) notes that these constants could be derived from relative density, D_r, as below:

$$c_1 = 7600 (D_r)^{-2.5} \qquad (6)$$

$$c_2 = \frac{0.4}{c_1} \qquad (7)$$

This definition is available in FLAC^{2D} as a built-in model (named Finn model) that incorporates Eq. (5) into the standard Mohr-Coulomb plasticity model. The Finn model is used in the present study for modeling of pore pressure generation during seismic analysis.

RESULTS AND COMPARISONS

Since initial shear stresses are known to affect both the stress-strain behavior and liquefaction resistance of sands, particular attention was given to the simulation and determination of initial geostatic conditions. Comparison between the corresponding computed and measured results (Computed: numerical and Measured: shaking table results) is presented and discussed in the following main outcomes:

Soil Acceleration Records in Free Field

Soil acceleration time histories in free field (for ACC2, ACC5, ACC6, and ACC7), for both computed and measured results are plotted in Figure 5. As can be observed in this figure, the amplitude of acceleration records decreases significantly at early stages of shaking, as the soil goes to be liquefied and consequently loses its shear strength. This type of response can be found accordingly from numerical simulation as well as the experiment. It was also resulted from the shake table test that the acceleration amplitudes in shallower depths (except ACC7, located on ground surface) decreased sooner than those corresponding to deeper soils. The computed results also conform this

manner pretty well, as the shallow soil liquefied sooner due to lower confining pressure. Minor amplification relative to the base motion was observed in the acceleration record at top of the lower non-liquefiable layer (ACC2), in both numerical and experimental results.

Excess Pore Water Pressure Time Histories

Pore water pressure transducers PWP4, PWP5, and PWP6 were located in free field while PWP1 and PWP2 were installed at upslope, adjacent to the pile 3, and PWP7 was placed at downslope side of it (Haeri et al., 2012). In the simulation, pore water pressure histories are specified to record at grid points that imitate the locations of installed PWP transducers in the test. The recorded excess pore pressure time histories by the test and computed by simulation (FLAC^{2D}), are shown in Figures 6 and 7, both for free field and closed to the pile, respectively. The reference values of pore water pressure for measured results are scaled to prototype that is written in the right side of the diagram. The measured and computed excess pore water pressure are fairly in a good agreement with each other. General trend of both calculation and measurement showed that the soil liquefied after about a few cycles of shaking in free field; and the upper transducer indicates liquefaction sooner. In the other hand, near the pile as it can be seen, upslope soil element located at PWP2 liquefied a little later. Haeri et al. (2012) construed this behavior so that the soil near the pile will constrained by the pile during the early stages of shaking, preventing it from experiencing enough shear strain and thus full liquefaction. The downslope soil element (located at PWP7) did not completely liquefy; they also interpreted it due to the separation of downslope soil from the pile and consequently formation of a drainage path.
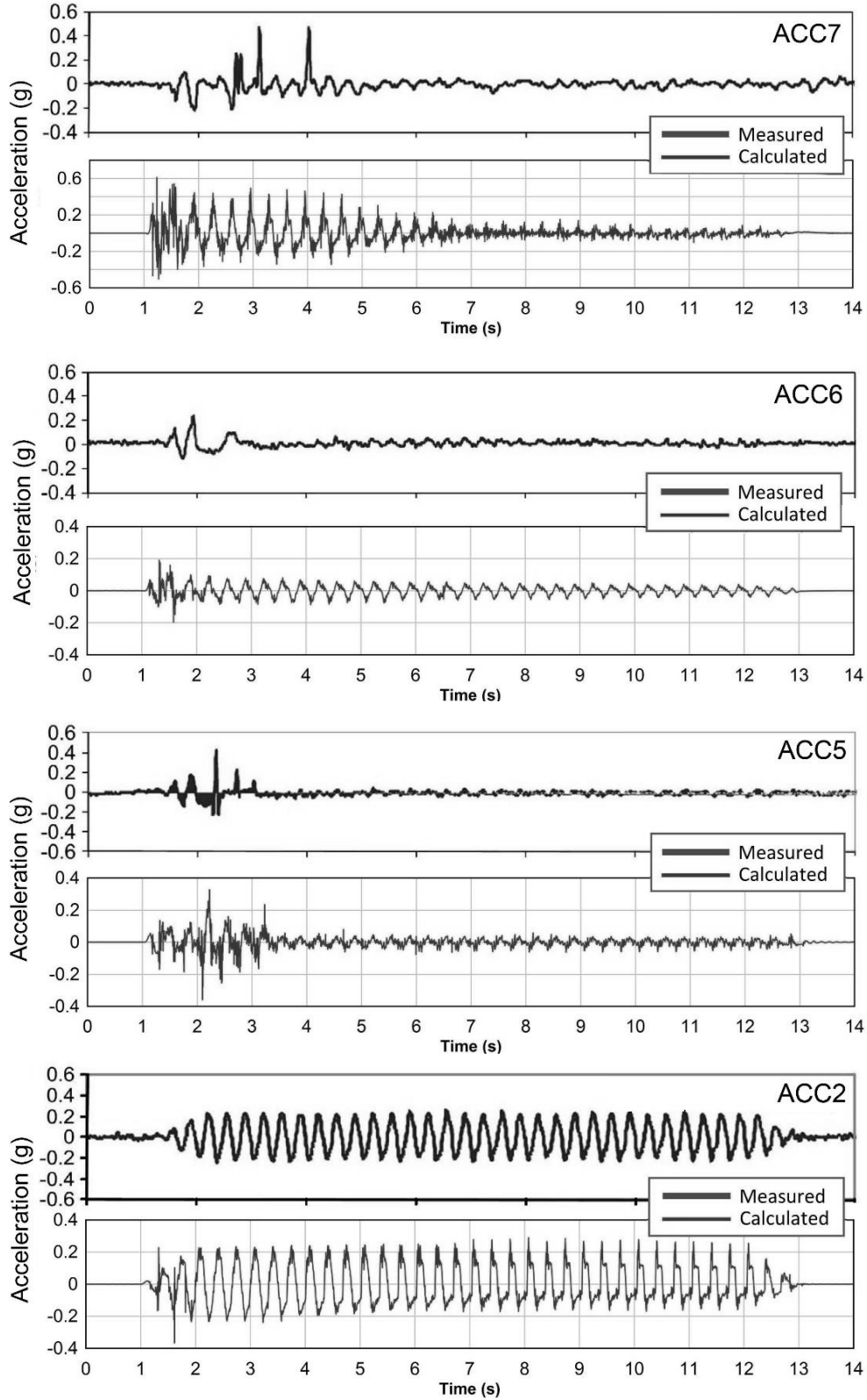
Fig. 5. Comparison of acceleration time histories of soil in free field for computed (FLAC[2D]) and measured (Haeri et al., 2012) results in different depths

Altogether, the numerical simulation shows to be able to model the soil liquefaction even by details. The controversial issue is related to after liquefaction stage that is the dissipation of excess water pressure (EPWP) after the seismic load. As can be seen in Figure 6b and Figure 7b, in the numerical simulation, the generated pore water pressure dissipates with a slower rate, so that even 20 s after the seismic load, the amount of EPWP is not reaching zero. This delayed dissipation could be interpreted by the fact that in real case (test), the structure of soil would be destroyed when liquefaction occurs and the permeability of liquefied soil might increase, but since the liquefied soil's permeability would not be automatically changed by FLAC^{2D} program, the permeability might be under-estimated after liquefaction compared to the real case. If this assumption is true, the permeability of the liquefied soil should be enlarged at dissipation stage of modeling. It is worth mentioning that some previous efforts have considered the permeability variation during liquefaction in their simulations, e.g., (Shahir et al., 2012, Rahmani et al., 2012).

Pile Head and Ground Surface Lateral Displacement

Comparisons of computed and measured results are presented in Figures 8 and 9 for ground surface and pile head displacements, respectively. The computed response was found to be in a good agreement with that observed in the experiment (Haeri et al., 2012), including the deformation pattern and maximum value. Lateral displacement time histories of the pile head (pile 3) and ground surface, computed from the simulation as well as the test results, show that the soil starts to move towards downslope when being liquefied a few seconds after beginning of the shaking.
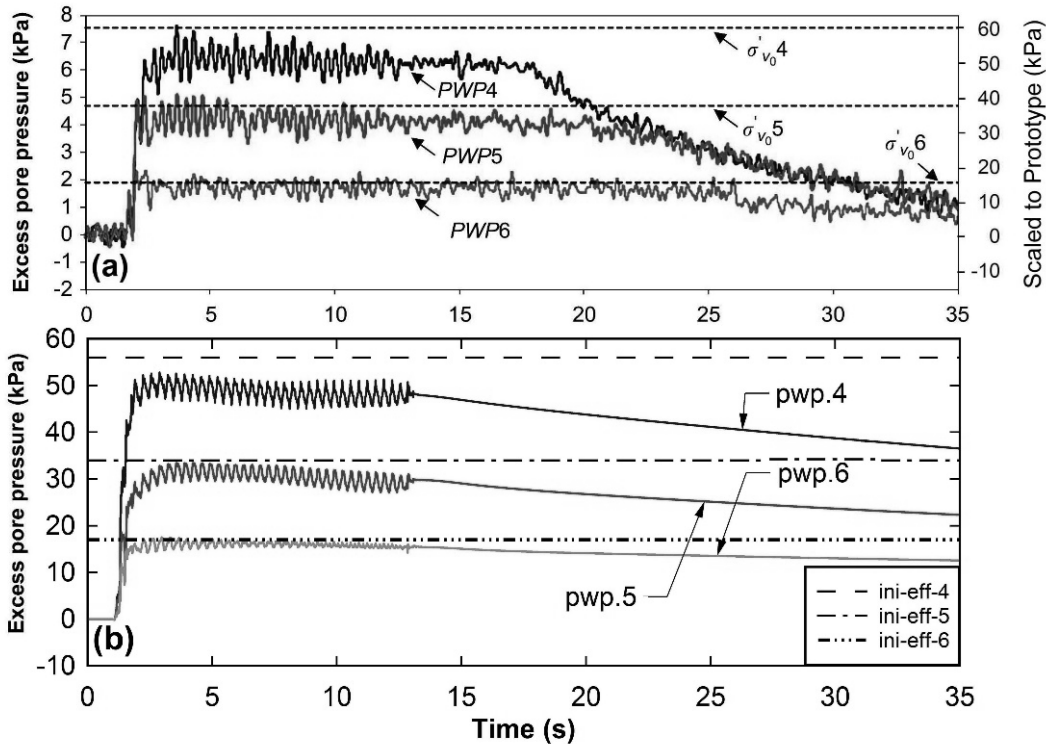

Fig. 6. Comparison of excess pore pressure time histories at free field: a) Measured by the test (Haeri et al., 2012), and b) Computed by simulation (FLAC^{2D})

It also indicates that the free field soil displacement keeps increasing until the end of the shaking but the pile head displacement reaches its maximum displacement a few seconds after the lateral spreading and then bounces back gradually (due to the pile's rigidity) as the shaking continues and a residual displacement remains at the end. It can be seen that the computed residual displacements of pile head at the end of shaking are a little greater than those for measured values.
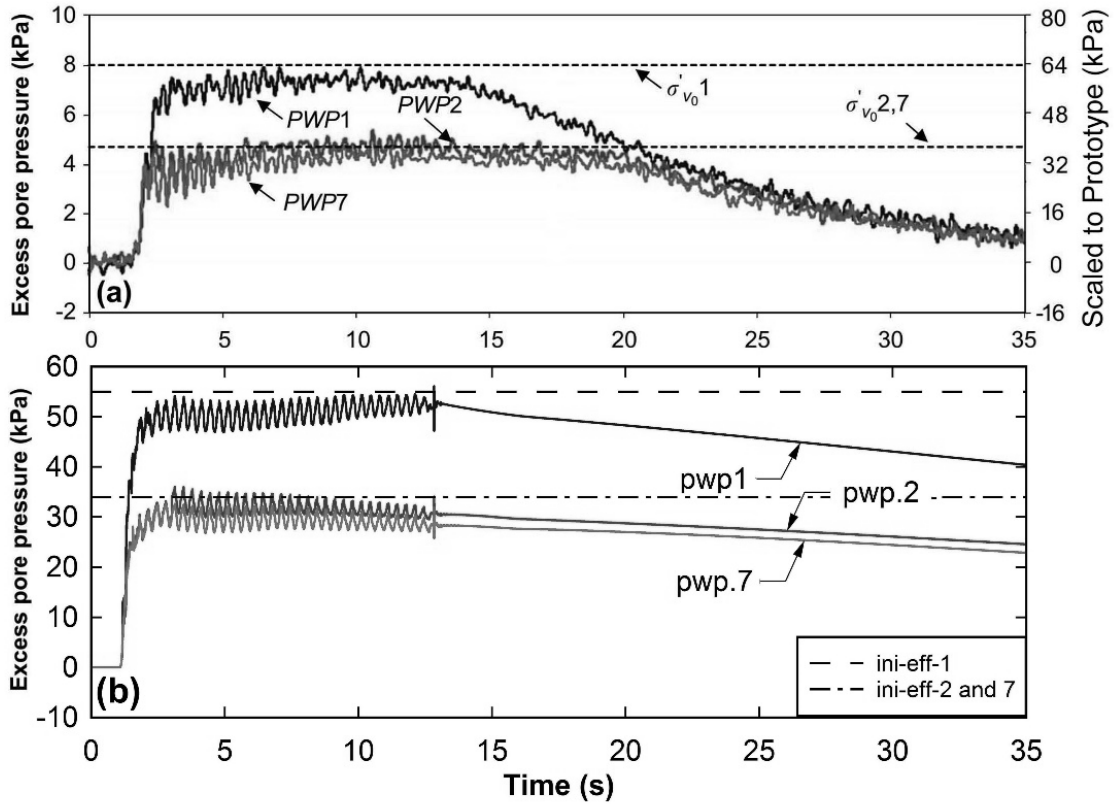

Fig. 7. Comparison of excess pore pressure time histories closed to the pile: a) Measured by the test (Haeri et al., 2012), b) Computed by simulation (FLAC^{2D})
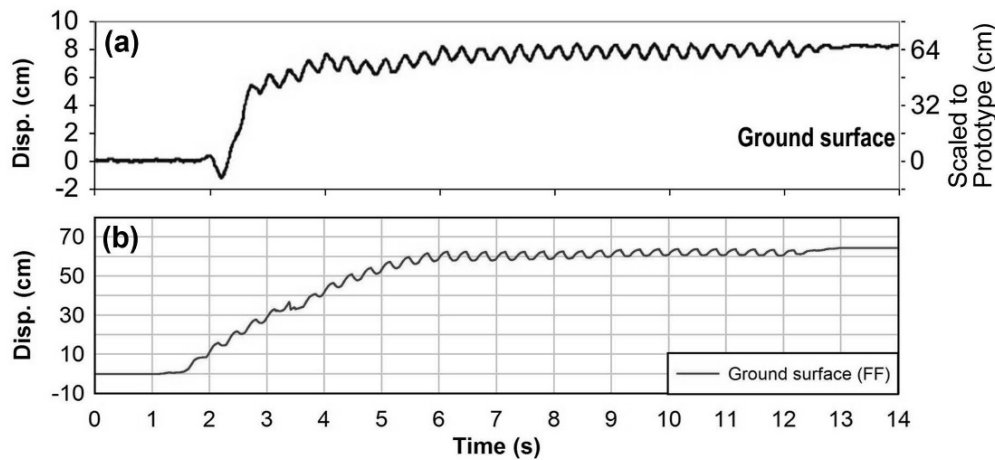

Fig. 8. Comparison of lateral displacement time histories of ground surface: a) Measured by the test (Haeri et al., 2012), b) Computed by simulation (FLAC^{2D})
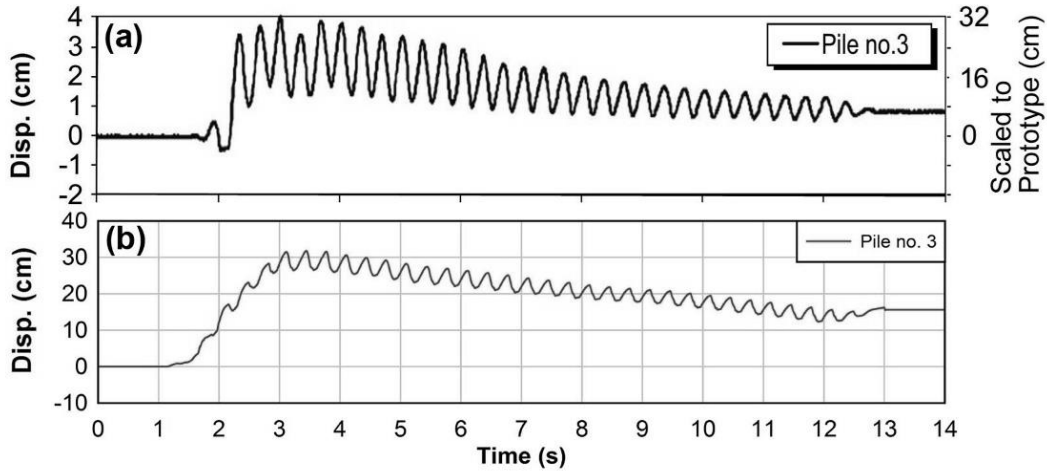
Fig. 9. Comparison of lateral displacement time histories of pile head (pile 3): a) Measured by the test (Haeri et al., 2012), b) Computed by simulation (FLAC^{2D})

Pile Bending Moment

The measured and computed time histories of bending moments for single pile (pile 3) at the base of the liquefied layer are shown in Figure 10, during dynamic loading. These time histories identically show that the bending moment reaches the maximum value a few seconds after the beginning of shaking (about $t = 3$ s), when the lateral spreading is occurred and displacement at the pile head is also maximum. Thereafter, as noted before, the pile starts to bounce back and accordingly bending moment is decreased gradually despite the fact that the liquefied soil keeps moving around the piles towards downslope. From the comparison of results, it is obtained that at the time of peak bending moment, the computed peak moment is generally smaller than measured value and also the computed bending moment does not reach zero at the end of shaking and a permanent moment remains. However, the bending moment was completely reduced and reached zero in the test.
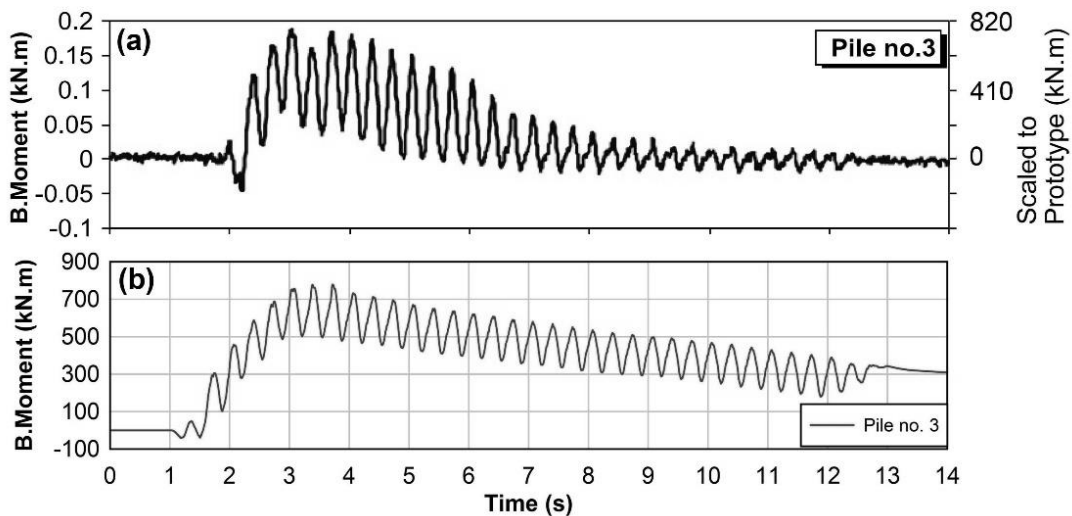

Fig. 10. Comparison of bending moment time histories of pile (pile 3) at the base of liquefied soil: a) Measured by the test (Haeri et al., 2012), b) Computed by simulation (FLAC^{2D})

Shadow and Neighboring Effects

As mentioned before, three different series of model piles were configured in the test (Haeri et al., 2012). Piles 1 and 2 as front and shadow piles were aligned in the direction of lateral spreading to study shadowing effect, while piles 4, 5, and 6 formed a set of three piles aligned in a row perpendicular to the direction of lateral spreading to study the neighboring effect. Similar group effects at various levels were also studied by Towhata et al. (2006). He et al. (2008) also observed that lateral spreading load on individual piles was a function of pile location in the pile group. In the present paper, the computed maximum bending moments and lateral forces (shear forces) exerted on each pile compared to pile 3 (as a single pile), are investigated to evaluate the power of the presented 2D plane strain numerical simulation (FLAC^{2D}) of 3D effects. As it was noted before, both shadow and neighboring effects in pile groups are 3D effects; therefore, the third dimension (in the direction perpendicular to the lateral spreading) of problems in 2D modeling is expected to lead to more unrealistic results.

Haeri et al. (2012) observed that the piles contributed in groups, experienced less forces and bending moments compared to a single pile. They defined a factor to assess the amount of this reduction. The reduction factor (RF) was calculated as: the reduction amount of maximum force/bending moment for each pile in group (compared to the single pile), over the maximum force/bending moment of the single pile (pile 3). Also in the numerical simulation, reduction factors for different piles are computed based on the above definition and are compared with the measured results, which are graphically shown in Figures 11 and 12 for bending moment and shear force, respectively. The results show that shadowing effect in piles 1 and 2 has been successfully simulated in the 2D analysis so that it reduced exerted forces in the front and downslope piles just like the test. However, for numerical modeling, the amount of this reduction in pile 2 (as a shadow pile) is a few percent greater than that measured by the test (5% and 11% for shear force and bending moment, respectively).
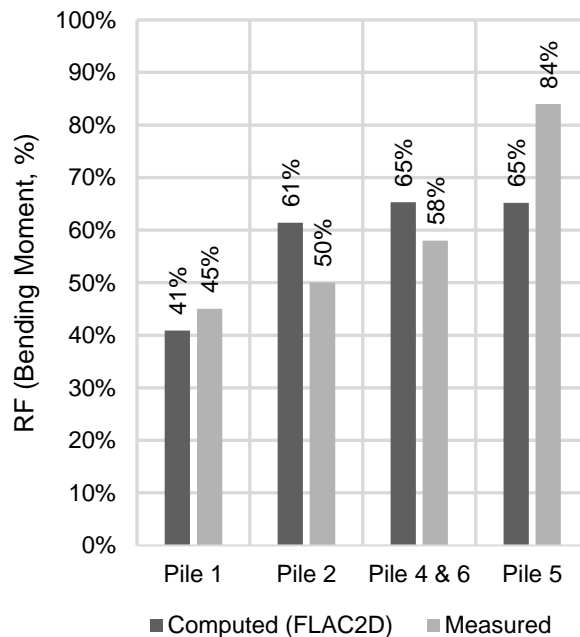

Fig. 11. Comparison of reduction in bending moment in different piles comparing to the single pile (pile 3) for computed (FLAC^{2D}) and measured (Haeri et al., 2012) results
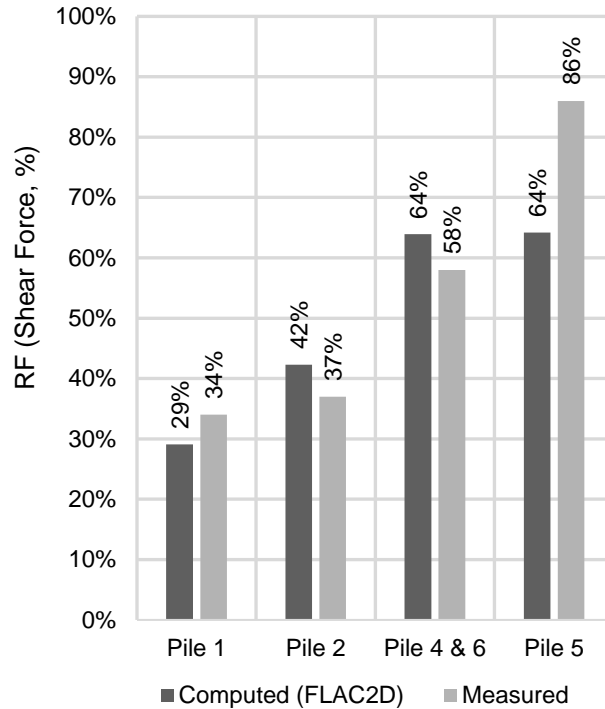
Fig. 12. Comparison of reduction in shear force in different piles comparing to the single pile (pile 3) for computed (FLAC^{2D}) and measured (Haeri et al., 2012) results

For pile 1 as a front pile, the reduction factor computed by numerical modeling is about 5 percent less than measured by the test.

Neighboring effect is also studied by calculating RF for piles 4, 5, and 6 (configured perpendicular to lateral spreading) using current numerical simulation. Since the piles are scaled in the simulation considering the method proposed by Donovan et al. (1984), in which they are represented by one equivalent pile, same results are going to be computed for all the three piles. In other words, the 2D modeling of neighboring effect in pile groups is capable of only computing an identical behavior for each pile aligning in the neighboring direction. Nevertheless, the results show that the computed RF in shear force and bending moment is seem to have an average amount between the values measured experimentally by Haeri et al. (2012) for each neigboring pile. It is interested to note that such an equivalence may be very helpful in the primary analysis of substantially 3D problems, saving time and difficulties. Comparison between computed and measured RF of neighboring piles is also depicted in Figures 11 and 12.

CONCLUSIONS

A nonlinear effective stress analysis incorporating an elastoplastic constitutive model based on Finite Difference method has been used to numerically simulate shaking table experiment on piles subjected to lateral spreading. Dynamic response of soil-pile foundation system and the capability of 2D numerical simulation of 3D effects such as shadow and neighboring effects in pile groups without a pile cap were evaluated. Based on this study, the following major conclusions can be drawn:

1. The Finite Difference method using the program FLAC^{2D} and the constitutive model Finn are generally capable of reproducing the primary features of the shaking table test, such as the acceleration

response, patterns of displacements, and the relative differences between the pile head and ground surface displacements.

2. In the numerical simulation, the generated pore water pressure dissipates with a slower rate, so that it could be interpreted that permeability would not automatically changed by FLAC^{2D} program and it might be under-estimated after liquefaction, compared to real condition.

3. The simulation tends to under-predict the maximum bending moment during the dynamic loading while a residual bending moment was observed at the end of shaking.

4. Shadow and neighboring effects are modeled in the 2D simulation, although for numerical modeling, RF is a few percent over-predicted for the shadow pile (pile 2) and under-predicted for the front pile (pile 1). In the case of neighboring effect, it is observed that 2D simulation is only able to reduce the forces and moments generally, not in details, and the RF computed by simulation is approximately an average of measured RF between all neighbor piles.

5. Future studies are needed to further investigate and quantify the efficacy of 2D numerical simulation of 3D problems.

ACKNOWLEDGEMENTS

REFERENCES

Abdoun, T., Dobry, R., Zimmie, T.F. and Zeghal, M. (2005). "Centrifuge research of countermeasures to protect pile foundations against liquefaction-induced lateral spreading", *Journal of Earthquake Engineering,* 9 (sup001), 105-125.

Asaadi, A. and Sharifipour, M. (2015). "Numerical simulation of liquefaction susceptibility of soil interacting by single pile", *International Journal of Mining and Geo-Engineering,* 49(1), 47-56.

Askari, F., Dabiri, R., Shafiee, A. and Jafari, M.K. (2011). "Liquefaction resistance of sand-silt mixtures using laboratory based shear Wave velocity", *International Journal of Civil Engineering,* 9(2), 135-144.

Byrne, P.M. (1991). "A cyclic shear-volume coupling and pore pressure model for sand", *Proceedings of the 2nd International Conference on Recent Advances in Geotechnical Earthquake Engineering and Soil Dynamics*, St. Louis.

Byrne, P.M., Park, S.-S., Beaty, M., Sharp, M., Gonzalez, L. and Abdoun, T. (2004). "Numerical modeling of liquefaction and comparison with centrifuge tests", *Canadian Geotechnical Journal,* 41(2), 193-211.

Chang, D., Boulanger, R., Brandenberg, S. and Kutter, B. (2013). "FEM analysis of dynamic soil-pile-structure interaction in liquefied and laterally spreading ground", *Earthquake Spectra*, 29(3), 733-755.

Cheng, Z. and Jeremić, B. (2009). "Numerical modeling and simulation of pile in liquefiable soil", *Soil Dynamics and Earthquake Engineering, 29*(11), 1405-1416.

Dabiri, R., Askari, F., Shafiee, A. and Jafari, M. (2011). "Shear wave velocity-based liquefaction resistance of sand-silt mixtures: Deterministic versus probabilistic approach", *Iranian Journal of Science and Technology Transaction B: Engineering,* 35(C2), 199-215.

Donovan, K., Pariseau, W. and Cepak, M. (1984). "Finite Element approach to cable bolting in steeply dipping VCR slopes", *Geomechanics Application in Underground Hardrock Mining,* 65-90.

Haeri, S. M., Kavand, A., Rahmani, I. and Torabi, H. (2012). "Response of a group of piles to liquefaction-induced lateral spreading by large scale shake table testing", *Soil Dynamics and Earthquake Engineering,* 38, 25-45.

He, L., Elgamal, A., Hamada, M. and Meneses, J. (2008). "Shadowing and group effects for piles during earthquake-induced lateral spreading", *Proceedings of the 14th World Conference on Earthquake Engineering,* Beijing, China.

Iai, S., Tobita, T. and Nakahara, T. (2005). "Generalised scaling relations for dynamic centrifuge tests", *Geotechnique,* 55(5), 355-362.

Itasca Consulting Group, I. (2011). *FLAC-fast Lagrangian analysis of continua*, *User's manual*, *version 7.0*, Minneapolis.

Karimi, Z. and Dashti, S. (2015). "Numerical and centrifuge modeling of seismic soil–foundation–structure interaction on liquefiable ground",

Journal of Geotechnical and Geoenvironmental Engineering, 142(1), 04015061.

Kuhlemeyer, R.L. and Lysmer, J. (1973). "Finite Element method accuracy for wave propagation problems", *Journal of Soil Mechanics and Foundations Division,* 99(SM5), (Technical Report).

Mirlatifi, S.A., Fakher, A. and Ghalandarzadeh, A. (2007). "Seismic study of reinforced earth walls by shaking table model tests", *In 4th International Conference on Earthquake Geotechnical Engineering*, Paper No. 1253.

Oberkampf, W.L., Trucano, T.G. and Hirsch, C. (2004). "Verification, validation, and predictive capability in computational engineering and physics", *Applied Mechanics Reviews,* 57(5), 345-384.

Popescu, R. and Prevost, J.H. (1993). "Centrifuge validation of a numerical model for dynamic soil liquefaction", *Soil Dynamics and Earthquake Engineering,* 12(2), 73-90.

Rahmani, A., Fare, O.G. and Pak, A. (2012). "Investigation of the influence of permeability coefficient on the numerical modeling of the liquefaction phenomenon", *Scientia Iranica,* 19(2), 179-187.

Rahmani, A. and Pak, A. (2012). "Dynamic behavior of pile foundations under cyclic loading in liquefiable soils", *Computers and Geotechnics,* 40(March), 114-126.

Shahir, H., Pak, A., Taiebat, M. and Jeremić, B. (2012). "Evaluation of variation of permeability in liquefiable soil under earthquake loading", *Computers and Geotechnics,* 40, 74-88.

Su, L., Tang, L., Ling, X.Z., Ju, N. P. and Gao, X. (2015). "Responses of reinforced concrete pile group in two-layered liquefied soils: shake-table investigations", *Journal of Zhejiang University Science A*, 16(2), 93-104.

Tokimatsu, K., Oh-Oka, H., Shamoto, Y., Nakazawa, A. and Asaka, Y. (1997). "Failure and deformation modes of piles caused by liquefaction-induced lateral spreading in 1995 Hyogoken-Nambu earthquake", *Proceedings of the Third Kansai International Geotechnical Forum on Comparative Geotechnical Engineering.*

Tokimatsu, K., Suzuki, H. and Sato, M. (2005). "Effects of inertial and kinematic interaction on seismic behavior of pile with embedded foundation", *Soil Dynamics and Earthquake Engineering,* 25(7), 753-762.

Towhata, I., Sesov, V., Motamed, R. and Gonzalez, M. (2006). "Model tests on lateral earth pressure on large group pile exerted by horizontal displacement of liquefied sandy ground", *8th US National Conference on Earthquake Engineering,* San Francisco, California.

Wilson, D.W. (1998). "Soil-pile-superstructure interaction in liquefying sand and soft clay", PhD Thesis, University of California, Davis.